ISSN 0208-7774 TRIBOLOGIA 3/2023 p. 71–80
DOI: 10.5604/01.3001.0053.9438

Stanisław STRZELECKI[*], Dominik OLBRZYMEK[**], Jakub OLBRZYMEK[**]

STATIC CHARACTERISTICS OF 3-LOBE JOURNAL BEARINGS WITH DIFFERENT LOBES OF GEOMETRY

CHARAKTERYSTYKI STATYCZNE 3-POWIERZCHNIOWYCH ŁOŻYSK ŚLIZGOWYCH Z SEGMENTAMI RÓŻNEJ GEOMETRII

Key words: multilobe journal bearings, lobe geometry, static characteristics.

Abstract: The 3-lobe journal bearings have found application in high-speed bearing systems. The bearing design and the number of lobes and oil grooves ensure good cooling conditions for the bearings. These bearings can be manufactured as bearings with cylindrical, non-continuous operating surfaces separated by six lubricating grooves, bearings with a pericycloid shape of bearing bore and Offset ones.
This paper presents the results of the computation of static characteristics of the 3-lobe journal bearing with the lobes of different geometry. The conditions of an aligned axis of the journal and sleeve and the static equilibrium position of the journal were assumed. Different bearing length-to-diameter ratio values and relative and lobe relative clearance were considered. Reynolds' energy and viscosity equations were solved by means of an iterative procedure. Adiabatic oil film and laminar flow in the bearing gap were considered. It was stated that different lobe geometries generate changes in the characteristics of bearings.

Słowa kluczowe: smarowanie hydrodynamiczne, wielopowierzchniowe łożyska ślizgowe Offset, charakterystyki statyczne.

Streszczenie: Łożyska ślizgowe 3-powierzchniowe stosowane są w układach łożyskowania o dużej liczbie obrotów. Konstrukcja tych łożysk i liczba powierzchni ślizgowych oraz rowków smarowych zapewniają dobre warunki chłodzenia. Łożyska te mogą być wykonywane z segmentami o powierzchni kołowej, zarysie nieciągłym lub ciągłym; z przesuniętymi segmentami a powierzchnie ślizgowe są oddzielone rowkami smarowymi.
W artykule przedstawiono obliczenia charakterystyk statycznych łożysk 3-powierzchniowych z segmentami o różnej geometrii pracujących w warunkach równoległych osi czopa i panewki i statycznego położenia równowagi czopa. Założono różne wartości względnej długości łożyska, luzu łożyskowego i względnego luzu segmentu. Równanie Reynoldsa, energii i lepkości rozwiązano metodą różnic skończonych autorskim kodem numerycznym. Przyjęto adiabatyczny i laminarny model przepływu środka smarowego w szczelinie smarowej.

INTRODUCTION

Circular (cylindrical) journal bearings are widely used in many bearing arrangements. A simple shape, low manufacturing cost and the possibility of transferring significant loads characterise them. The limitation of using these bearings in rotating machines is the high temperature of the lubricating film and unstable operation in the range of higher rotational speeds.

In high-speed rotating machines, such as turbochargers, steam turbines, gas turbines and in turbine gearboxes, multilobe, radial (radial) plain bearings are used for various reasons with pressure lubricant supply, being hybrid bearings **[L. 1–11]**. These bearings provide favourable temperature conditions for the lubricating film, vibration-free operation, and damping of vibrations caused by unbalanced and self-excited oil vibrations **[L. 12, 13]**.

[*] ORCID 0000-0001-5030-5249, Łodź, Poland.
[**] LEDO S.c., Łódź, Poland.

Multilobe (surface), hydrodynamic and hybrid radial plain bearings are bearings with a sleeve of a non-circular bore consisting of several fixed (from 2 to 8) **[L. 2–8]** or tilting (essentially 3 to 5) **[L. 1–3]** of the sliding surfaces, each producing a hydrodynamic pressure, temperature and a viscosity field.

The known results of the research conducted so far on cylindrical and multilobe journal bearings consider to a small extent, the issue of the influence of the continuous or discontinuous shape of the sleeve bore **[L. 2, 4, 6]** on the static and dynamic characteristics of bearings **[L. 5, 12, 13]**.

At the Department of Machine Parts at the Lodz University of Technology in the 1970s, theoretical and experimental research was carried out on the influence of the continuous profile of bearing bore on the static and dynamic characteristics of multilobe bearings. The research was limited to a 3-lobe bearing with a pericycloid profile and the isothermal and adiabatic model of the lubricating film **[L. 2, 4]**.

The development of rotating machines in the direction of obtaining higher rotational speeds and power output, as well as higher reliability and durability, increases the requirements for static and dynamic characteristics of journal bearings **[L. 2, 6, 7, 9]**. Static characteristics define pressure, temperature and viscosity distribution in the lubricating film, hydrodynamic load capacity, static equilibrium angles, maximum pressure and temperature values, the minimum thickness of the lubricating film, power losses and lubricant flow **[L. 1–4].** The full characteristics of the journal bearing are determined in an iterative process for a specific position of the journal on the curve of static equilibrium positions.

Research centres conduct theoretical and experimental work on multilobe bearings, ensuring, in particular, an increase in load capacity and a reduction of power losses **[L. 5-10]**. Information on design and technological changes in order to obtain optimal operating conditions for 2-lobe high-power turbogenerator bearings is given in **[L. 6]**, where it was found that the load capacity increased by 25%. However, there is no information on the design details of the tested bearings.

The process of the design of multilobe, high-speed bearings operating at peripheral speeds from 20 to 200 ms^{-1} requires the correct determination of the viscosity and temperature **[L. 14–18]** of supplied lubricant and checking whether the minimum oil film thickness and its maximum temperature are within the permissible limits.

The surface pressure in this type of bearing is not high, i.e., the size of the lubricating gap is relatively large. Hence, new types of multilobe journal bearings should ensure new properties of bearings and bearings systems **[L. 2, 10]**. For example, a 3-lobe bearing can be designed as the classic multilobe or pericycloid one (**Fig. 1**; the area between the segment profile and the circle inscribed in the sleeve bore, marked in red, refers to a pericycloid bearing). Such a bearing geometry allows obtaining static and dynamic characteristics different from those of the classic multilobe bearing or pericycloid, in which the lobe has the same geometry.

Multilobe journal bearing can be composed of lobes of the same (**Fig. 1**) or different geometry (**Fig. 2**) **[L. 2, 10]**. In classic multilobe bearings, the lobes are characterised by circular profiles inscribed into the profile of the sleeve bore. So far, theoretical and experimental studies of multilobe bearings have lacked information on the static and dynamic characteristics of bearings with lobes of different geometry **[L. 2]**.

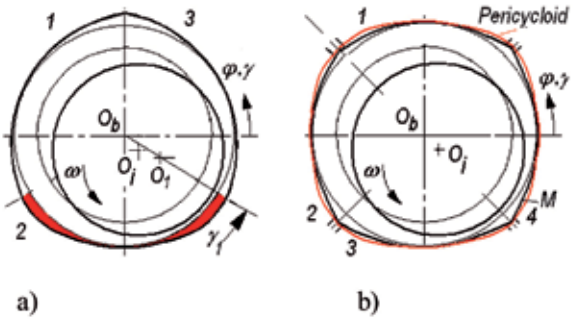

Fig. 1. Examples of 3- and 4-lobe journal bearings with the lobes of different geometry: a – 1,3 –multilobe M (non-continuous), 2 – pericycloid P (continuous), b – 4-lobe (M) and pericycloid (P): O_b, O_j, O_1 – centres of bearing, journal, lobe No.1), ω – angular velocity, coordinates: ϕ – peripheral, γ – lobe No. 1 centre

Rys. 1. Przykłady łożysk 3- i 4-powierzchniowych z segmentami o różnej geometrii: a – 1,3 –zarys wielopowierzchniowy (nieciągły), 2 – perycykloidalny (ciągły), b – 4-powierzchniowy klasyczny (M) i perycykloidalny (P); O_b, O_j, O_1 – środki: łożyska, czopa, segmentu nr 1), współrzędne: ϕ, γ – obwodowa, środka segmentu nr 1, ω – prędkość kątowa

This paper aims to obtain the newly desired properties of multilobe journal bearings and proposes using the lobes of different geometries in one multilobe bearing, e.g. circular, classic

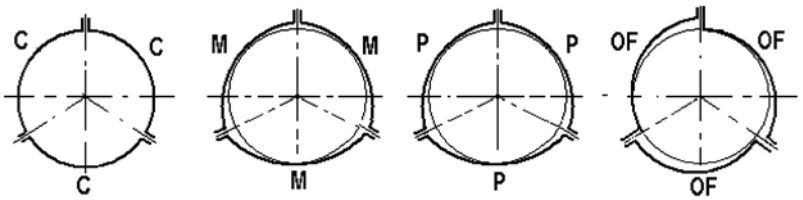

Fig. 2. 3-lobe journal bearings of different profiles of sleeve bore; C – cylindrical, M – multilobe, P – pericycloid, OF – Offset
Rys. 2. Łożyska 3-powierzchniowe z segmentami o różnej geometrii; C – cylindryczny, M – wielopowierzchniowy, P – perycykloidalny, OF – Offset

multilobe, pericycloid and Offset segments **[L. 2, 10]**. The design of such bearings leads to optimal static and dynamic characteristics, e.g., different temperature conditions of the lubricating film or a change in the resistance to motion (power losses). The assumptions of fluid film lubrication, incompressible Newtonian lubricant, no deformation of the bearing structure or the journal and parallel axes of the journal and sleeve were made.

BEARING GEOMETRY

The geometry of the lubricating film of multilobe journal bearings can be described by the general equation (1) **[L. 2, 4, 10]**.

$$\overline{H}(\varphi, z) = \overline{H}_C + \overline{H}_{M,P}(\varphi) \tag{1}$$

where: $\overline{H}_C$, $\overline{H}_{M,P}(\varphi)$ – the thickness of the lubrication gap for cylindrical and multilobe classic or pericycloid bearings, respectively (index: $_M$ – multilobe, $_P$ – pericycloid.

The first term of the right-hand side of the equation (1) determines the thickness of the lubricating gap for the eccentric position of the journal in the cylindrical bearing:

$$\overline{H}_C = 1 - \varepsilon \cos(\varphi - \alpha) \tag{2}$$

where: ε – eccentricity, α – attitude angle.

The geometry of the lubricating film of bearing with a pericycloid ("wave") profile and for a multilobe bearing **[L. 2, 3, 14]** with a concentric position of the journal axis and the sleeve is expressed non-dimensionally by the equations:

$$\overline{H}_P = \lambda^* (1 + cosn_p\varphi) \tag{3}$$

where: n_p – multiple of pericycloid, λ^* – pericycloid relative eccentricity

$$\overline{H}_M(\varphi) = \psi_s + (\psi_s - 1)\cos(\varphi - \gamma) \tag{4}$$

with ψ_s – segment clearance ratio $\psi_s = \overline{H}_{max} / \overline{H}_{min}$).

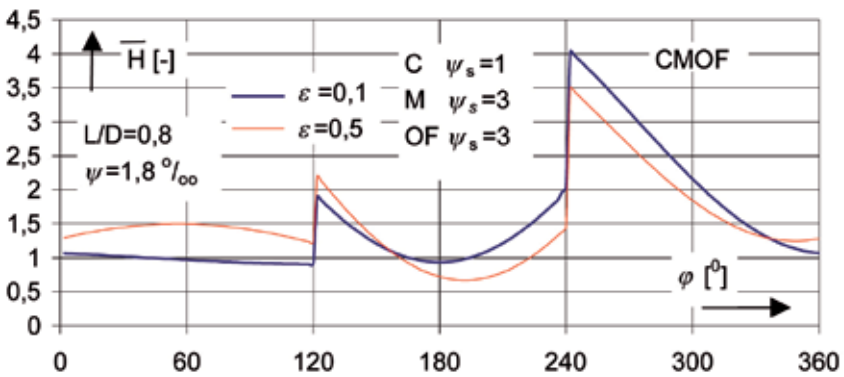

Fig. 3. The dimensionless oil film thickness of a 3-lobe journal bearing with the lobes of different geometry; C – cylindrical, M – multilobe, OF – Offset [L. 2]
Rys. 3. Bezwymiarowa grubość filmu smarowego łożyska 3-powierzchniowego z segmentami o różnej geometrii; C – cylindryczny, M – wielopowierzchniowy, OF – Offset **[L. 2]**

The dimensionless oil film thickness of a 3-lobe journal bearing with the lobes of different geometry and calculated at two values of journal relative eccentricity ε is shown in **Fig. 3**.

Numerical calculations of these bearings include the geometry parameters, such as the relative eccentricity of the lobe ψ_s and pericycloid λ^* and the values should allow for obtaining the proper characteristics of the considered bearing. In this case, the dependencies do not exist as in the case of an Offset type of bearing.

The dimensionless thickness of the lubricating gap of a 3-lobe journal bearing with the lobes that are composed of classic multilobe and pericycloid profiles is presented in **Fig. 4**; different values of the relative eccentricity of the journal were assumed; in the case of $\varepsilon = 0.03$ the centre of the journal is close to the centre of the sleeve, and the profiles are symmetric with regards to the line connecting the centres of lobe and sleeve (thick lines in **Fig. 4**).

The relationship determining the number of configurations of selected multilobe bearings was

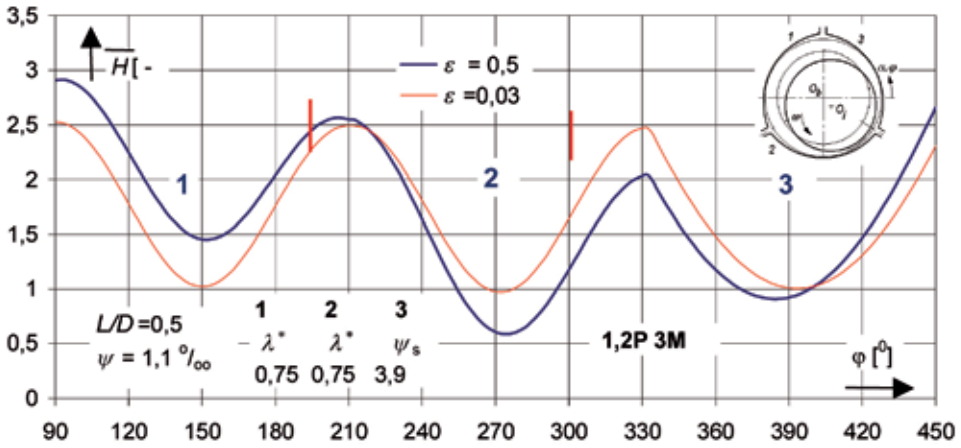

Fig. 4. The dimensionless thickness of the lubricating gap of a 3-lobe journal bearing with the lobes of different geometry; M – multilobe, P – pericycloid [L. 2]

Rys. 4. Bezwymiarowa grubość filmu smarowego łożyska 3-powierzchniowego z segmentami o różnej geometrii; M – wielopowierzchniowy, P – perycykloidalny **[L. 2]**

developed by Strzelecki **[L. 2,10]**. Exemplary, for a 3-lobe bearing and taking into account four basic bearing types, such as cylindrical C, multilobe M, pericycloid P and Offset OF, the number of possible lobes (sliding surfaces) geometries is 64 **[L. 2]**.

OIL FILM PRESSURE AND TEMPERATURE DISTRIBUTIONS

Oil film pressure, temperature and viscosity distributions can be computed by the coupled solution of geometry, Reynolds, energy and viscosity equations **[L. 2, 10]**. The oil film pressure field describes the following form of the Reynolds equation:

$$\frac{\partial}{\partial \varphi}\left(\frac{\overline{H}^3}{\eta}\frac{\partial \overline{p}}{\partial \varphi}\right)+\left(\frac{D}{L}\right)^2\frac{\partial}{\partial \overline{z}}\left(\frac{\overline{H}^3}{\overline{\eta}}\frac{\partial \overline{p}}{\partial \overline{z}}\right)=6\frac{\partial \overline{H}}{\partial \varphi}+12\frac{\partial \overline{H}}{\partial \phi} \tag{5}$$

where: $\overline{H}$ = h/(R-r) – dimensionless oil film thickness, h – oil film thickness (μm), $\overline{p}$ – dimensionless oil film pressure, $\overline{p} = p\psi^2/(\eta\omega)$, p – oil film pressure (MPa), r – journal radius (m), D, L – bearing diameter and length (m), R – sleeve radius (m), t – time (sec), ϕ, $\overline{z}$ – peripheral and axial co-ordinates, $\varphi = \omega\, t$ – dimensionless time, $\overline{\eta}$ – dimensionless viscosity, ψ – bearing relative clearance, $\psi = \Delta R/R$ (‰), ΔR – bearing clearance, $\Delta R = R - r$ (m).

$$\frac{\overline{H}}{Pe}\left[\frac{\partial^2\overline{T}}{\partial\varphi^2}+\left(\frac{D}{L}\right)^2\frac{\partial^2\overline{T}}{\partial\overline{z}^2}\right]+\left[\frac{\overline{H}^3}{12\eta}\frac{\partial\overline{p}}{\partial\varphi}-\frac{\overline{H}}{2}\right]\frac{\partial\overline{T}}{\partial\varphi}+\left(\frac{D}{L}\right)^2\frac{\overline{H}^3}{12\overline{\eta}}\frac{\partial\overline{p}}{\partial\overline{z}}\frac{\partial\overline{T}}{\partial\overline{z}}=$$
$$-\frac{\overline{H}^3}{12\overline{\eta}}\left[\left(\frac{\partial\dot{p}}{\partial\varphi}\right)^2+\left(\frac{D}{L}\right)^2\left(\frac{\partial\overline{p}}{\partial\overline{z}}\right)^2\right]-\frac{\overline{\eta}}{\overline{H}} \tag{6}$$

where: $\overline{T}$ – dimensionless oil film temperature, $\overline{T} = T/T_0$, Pe – Peclet number, $Pe = \rho c_t \omega r^2/\lambda$, ρ: oil density (kg/m^3), c_t: oil specific heat, (J/kgK), λ – heat transfer coefficient (W/m^{2}K).

It has been assumed for the pressure region that on the bearing edges, the oil film pressure $p(\varphi, z) = 0$ and in the regions of negative pressure, $p(\varphi, z) = 0$. The oil film pressure distribution computed from Eq. (5) has been introduced in the transformed energy equation **[L. 6]**. Temperature values $T(\varphi\pm, z)$ on the boundaries ($z = \pm L/2$) were determined by the mean of the parabolic approximation **[L. 2, 4, 12]**. Temperature and viscosity distribution were found by the iterative solution of equations (1) through (6), including the energy one **[L. 8]**.

RESULTS OF THE INVESTIGATION

The static characteristics determined in this paper included: displacement of the journal, angles of the static equilibrium position of the journal, oil film pressure, temperature, oil flow and power losses.

Exemplary results are given in **Fig. 5** through **Fig. 18**. It was assumed that the bearing length to diameter ratios are L/D = 0.64 and L/D = 0.8, and relative clearance of bearing was ψ = 1.8‰ with different lobe relative clearances ψ_s. The rotational speed of the journal was 3000 rpm, and the supplied oil temperature was $T_0 = 40^0$C.

Dimensionless oil film temperature distributions of 3-lobe journal bearings with the lobes of different geometry (C – cylindrical, M – multilobe, OF– Offset) are shown in **Fig. 5**. Different arrangement of the lobes causes the differences in the oil film temperature distributions; the largest difference as compared to the classic 3-lobe bearing (MMM – lobes with the same geometry) is observed on the 2nd and particularly on the 3rd lobe (the temperatures are higher for classic 3-lobe bearing than in 3-lobe bearing with the lobes of different geometry (CMOF). The temperature on the first, slightly loaded lobe is higher for the bearing with the lobe of different geometry

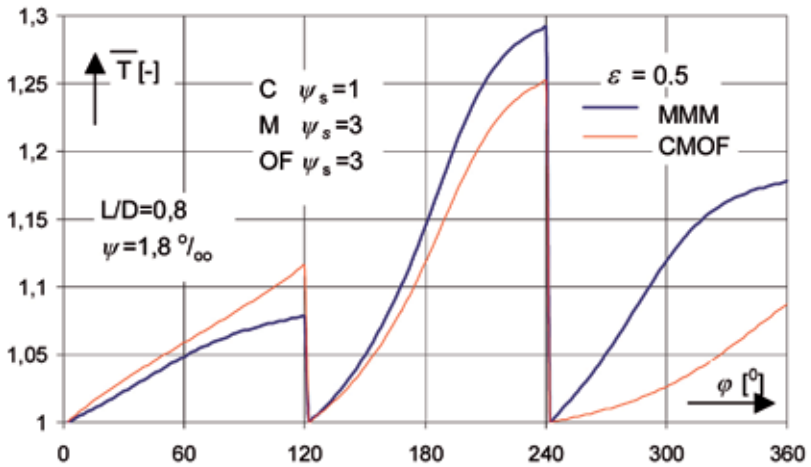

Fig. 5. Dimensionless oil film temperature distribution of a 3-lobe journal bearing with the lobes of different geometry; C – cylindrical, M – multilobe, OF – Offset

Rys. 5. Bezwymiarowa temperatura filmu smarowego łożyska 3-powierzchniowego z segmentami o różnej geometrii; C – cylindryczny, M – wielopowierzchniowy, OF – Offset

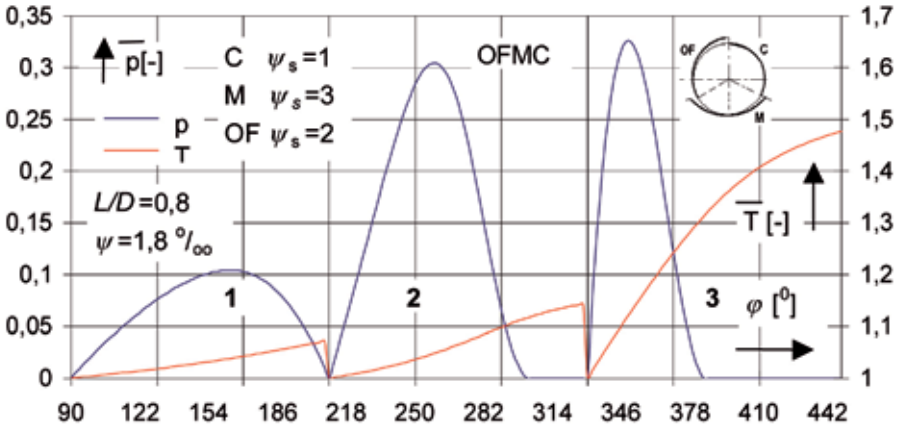

Fig. 6. The dimensionless oil film pressure and temperature distributions of a 3-lobe journal bearing with the lobes of different geometry; OF– Offset, M – multilobe, C – cylindrical

Rys. 6. Bezwymiarowe rozkłady ciśnienia i temperatury filmu smarowego łożyska 3-powierzchniowego z segmentami o różnej geometrii; OF– Offset, M – wielopowierzchniowy, C – cylindryczny

(**Fig. 6**, the angles from 0^0 through 120^0 of the 1st lobe).

For the 3 – lobe bearing with different lobes geometry (OF – Offset, M – multilobe, C – cylindrical), the dimensionless oil film pressure and temperature distributions can be observed in **Fig. 6**. Three different values of lobe relative eccentricity were considered (the profiles of bearing lobes: cylindrical ψ_s = 1, classic multilobe ψ_s = 3 and Offset ψ_s = 2). At assumed relative eccentricity ε the oil film pressure has the largest values on the 2nd and 3rd lobes. The highest temperatures shows the 3rd lobe, but the 1st and 2nd lobes have the lowest temperatures (**Fig. 6**). The smallest values of pressure and temperature are observed on the 1st lobe with an Offset profile, while the largest oil film pressures are on the 2nd and 3rd lobes (the lobes with classic multilobe M and cylindrical C geometry). Such a situation can be explained by the characteristics of cylindrical and Offset bearings; the first is used for high load and lower speeds (because among other high temperatures of operation), and the second is in the bearings systems with a smaller load and higher speeds (lower temperatures of operation).

Journal displacement and static equilibrium position angle versus Sommerfeld number S_0 ($S_0 = F \cdot \psi^2/(L \cdot D \cdot \eta \cdot \omega)$ where: F – static load of bearing in N) are shown in **Fig. 7** and **Fig. 8**, respectively. Two types of 3-lobe bearings were assumed, i.e., classic bearing (3M) and the bearing with different lobes geometry (1st and 3rd lobe – classic multilobe and the 2nd lobe – cylindrical profile). In both cases, the range of Sommerfeld's number is smaller for a classic 3-lobe bearing than in the case of a 3-lobe bearing with different lobes geometry (**Fig. 7** and **Fig. 8** – the range of Sommerfeld number is about 0.4 for classic 3-lobe bearing and 1, 2 for the bearing with different lobes geometry). However, the displacement of journal ε is larger for the classic 3-lobe bearing for the Sommerfeld numbers up to 0.1, but from this value, the displacements are smaller for the classic 3-lobe bearing. The static equilibrium position angles are larger for the classic 3-lobe bearing than in the case for the bearing with different lobes geometry (**Fig. 8**).

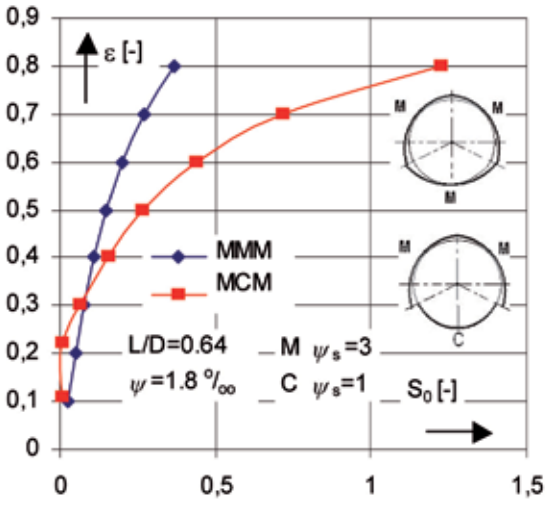

Fig. 7. Journal displacement versus Sommerfeld number for 3M journal bearings

Rys. 7. Przemieszczenie czopa w funkcji liczby Sommerfelda dla łożysk 3M i MCM

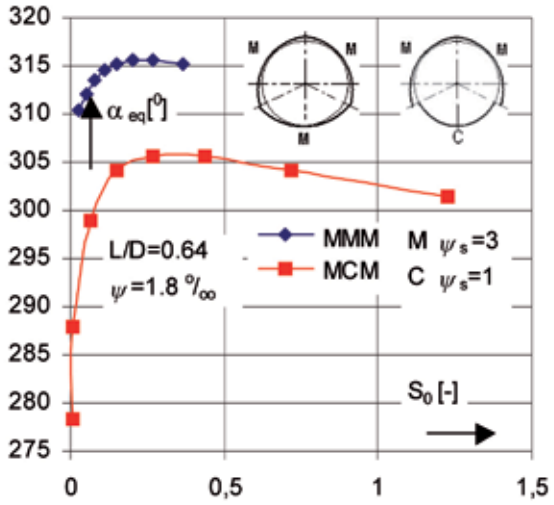

Fig. 8. Static equilibrium position angle versus Sommerfeld number for 3M and MCM journal bearings

Rys. 8. Kąty statycznego położenia równowagi w funkcji liczby Sommerfelda dla łożysk 3M i MCM

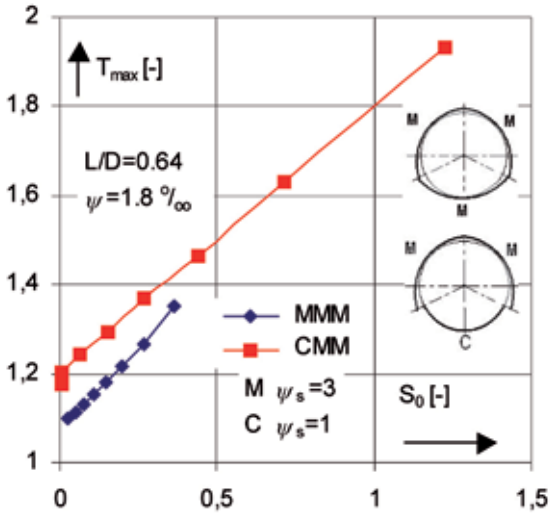

Fig. 10. Maximum oil film temperature of 3M and MCM journal bearings versus Sommerfeld number

Rys. 10. Maksymalna temperatura filmu smarowego łożysk 3M i MCM w funkcji liczby Sommerfelda

The minimum oil film thickness and maximum oil film temperature of classic 3-lobe (3M) and three lobes of different geometry (MCM) are given in **Fig. 9** and **Fig. 10.**

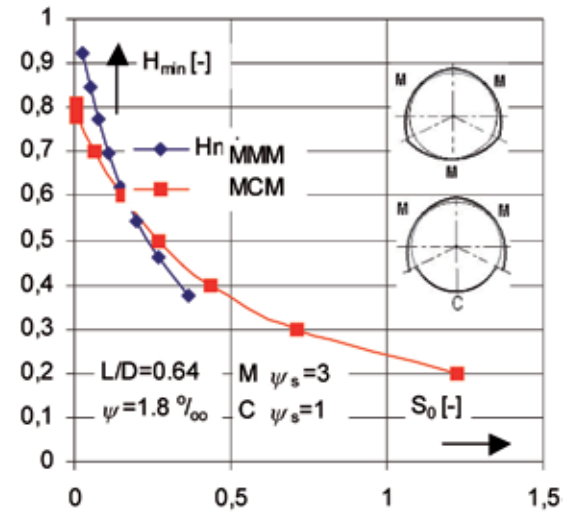

Fig. 9. Minimum oil film thickness of 3M and MCM journal bearings versus Sommerfeld number

Rys. 9. Minimalna grubość filmu smarowego łożysk 3M i MCM w funkcji liczby Sommerfelda

The oil flow and power losses of the 3-lobe classic bearing and 3-lobe bearing with the lobes of different geometry (1st and 3rd lobe as classic multilobe and the 2nd as cylindrical lobe) are shown in **Fig. 11** and **Fig. 12;** both parameters are calculated in function of Sommerfeld number. There is a larger difference in oil flow for the considered bearings, as it results from **Fig. 11**. The oil flow is larger for the classic bearing than in the bearing with the lobes of different geometry **(Fig. 11**). However, no significant difference is in power losses and particularly in smaller values of Sommerfeld numbers (**Fig. 12**).

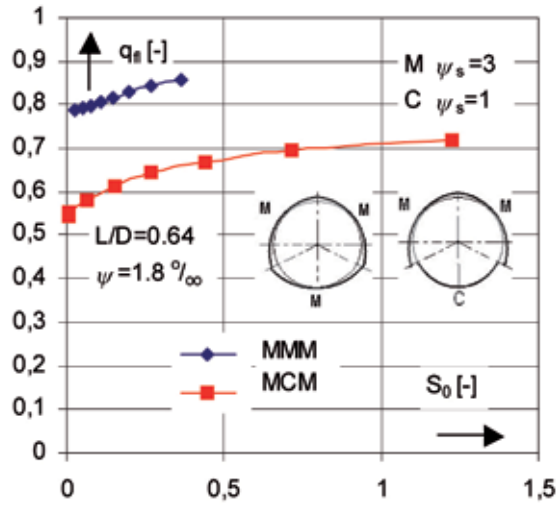

Fig. 11. Oil flow of 3M and MCM journal bearings versus Sommerfeld number

Rys. 11. Przepływ środka smarowego dla łożysk 3M i MCM w funkcji liczby Sommerfelda

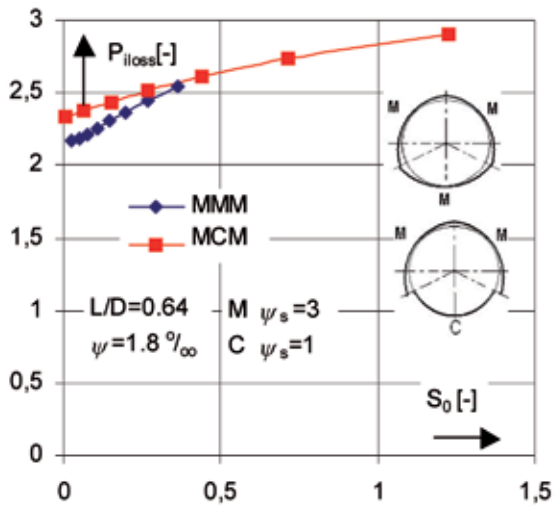

Fig. 12. Power loss of 3M and MCM journal bearings versus Sommerfeld number

ys. 12. Straty mocy łożysk 3M i MCM w funkcji liczby Sommerfelda

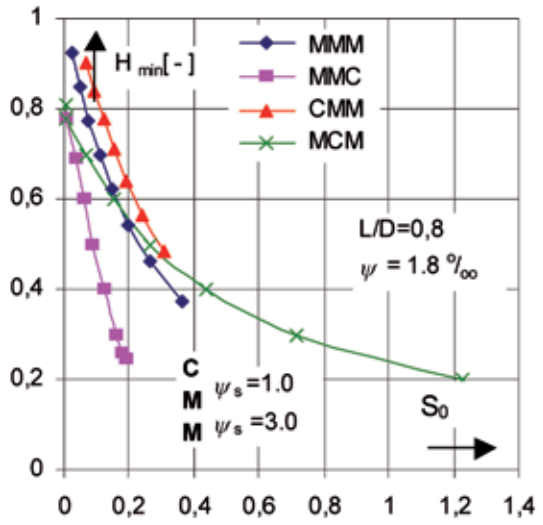

Fig. 13. Minimum oil film thickness of different 3-lobe journal bearings versus Sommerfeld number

Rys. 13. Minimalna grubość filmu smarowego dla różnych łożysk 3-powierzchniowych w funkcji liczby Sommerfelda

Minimum oil film thickness and static equilibrium position angle of different 3-lobe journal bearings are given in **Fig. 13** and **Fig. 14**, respectively, for a different arrangement of the geometry of lobes using the function of Sommerfeld's number. The relative clearance of the lobe was assumed as ψ_s = 1 for the lobe of and cylindrical profile and ψ_s = 3 for multilobe profile. It results from the diagrams that different arrangement of the geometry of lobes affects both minimum oil film thickness and static equilibrium position angles. Exemplary, minimum oil film thickness has the lowest values for the bearing with the lobes MMC (**Fig. 13**, 1st and 2nd lobes as classic multilobe, and the 3rd as cylindrical).

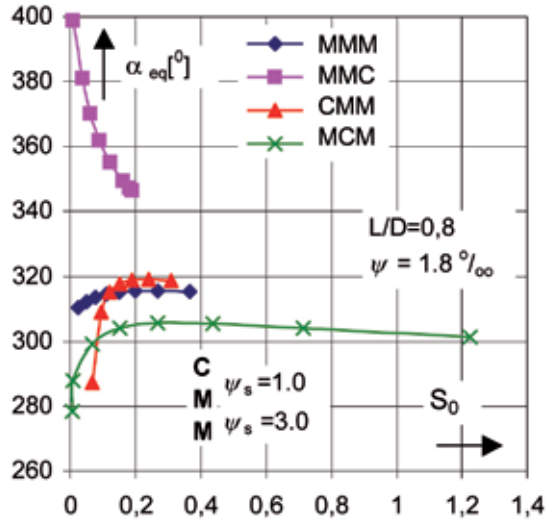

Fig. 14. Static equilibrium position angle of different 3-lobe journal bearings versus Sommerfeld number

Rys. 14. Kąty statycznego położenia równowagi dla różnych łożysk 3-powierzchniowych w funkcji liczby Sommerfelda

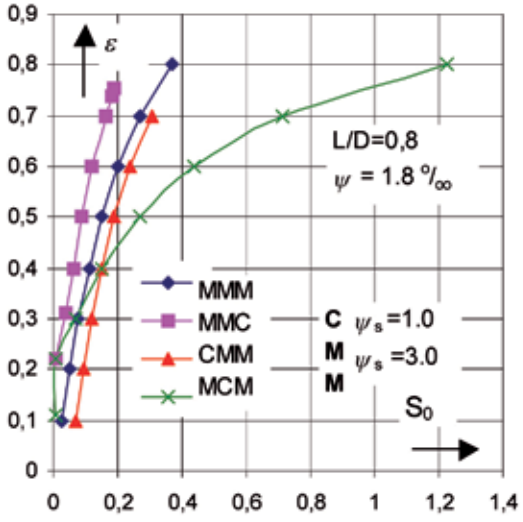

Fig. 15. Journal displacement of different 3-lobe journal bearings versus Sommerfeld number

Rys. 15. Przemieszczenie czopa dla różnych rodzajów łożysk 3-powierzchniowych w funkcji liczby Sommerfelda

Computed journal displacements (**Fig. 15**) and maximum oil film temperatures (**Fig. 16**) of four types of different 3-lobe journal bearings versus Sommerfeld number certify an effect of the different lobe geometry on the considered bearing parameters.

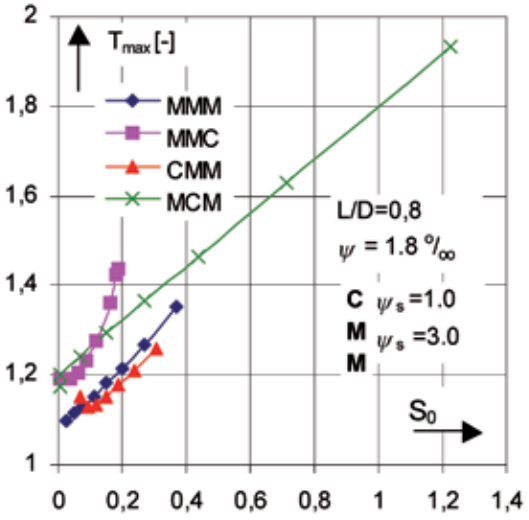

Fig. 16. Maximum oil film temperature of 3-lobe journal bearings versus Sommerfeld number

Rys. 16. Maksymalna temperatura filmu smarowego łożysk 3-powierzchniowych w funkcji liczby Sommerfelda

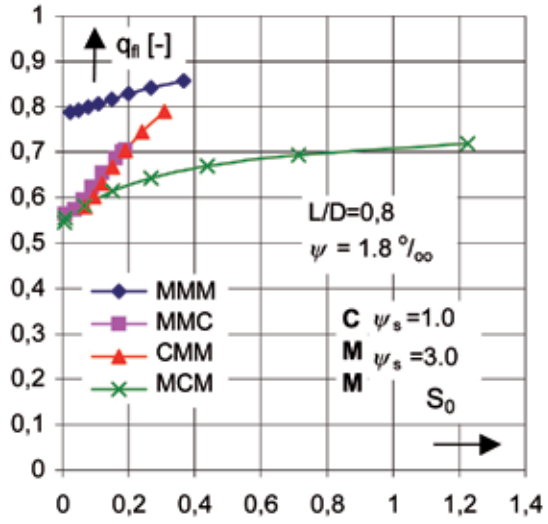

Fig. 17. Oil flow for different 3-lobe journal bearings versus Sommerfeld number

Rys. 17. Przepływ środka smarowego dla różnych łożysk 3-powierzchniowych w funkcji liczby Sommerfelda

Oil flow and power loss for different 3-lobe journal bearings can be observed in **Fig. 17** and **Fig. 18** versus Sommerfeld's number. These diagrams show the effect of different lobe configurations on the bearing parameters of operation. The smallest oil flow shows the bearing with lobes configuration MCM (**Fig. 17**, 1st and 3rd lobes as classic multilobe and the 2nd of a cylindrical profile). However, the lowest power loss is observed in the case of bearing MMM (**Fig. 18**, all lobes as classic multilobe).

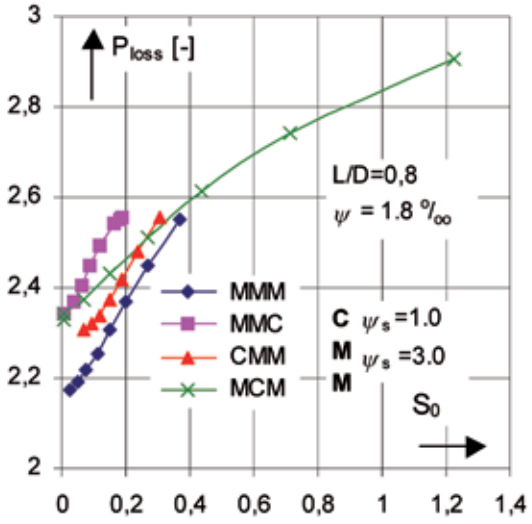

Fig. 18. Power loss for different journal bearings versus Sommerfeld number

Rys. 18. Straty mocy dla różnych łożysk 3-powierzchniowych w funkcji liczby Sommerfelda

FINAL REMARKS

The development and modifications of the numerical algorithm through the changes in bearings profiles enable the determination of the static characteristics of multilobe bearings with lobes of different geometry. It creates the possibility for designing a wide family of multilobe journal bearings characterised by new static and dynamic characteristics that are not currently applied.

The obtained results point to the variations of bearing characteristics according to the different geometry of the lobes in one bearing.

Analysis of the obtained results in the form of static characteristics of different configurations of multilobe bearings allows the designers to select them in accordance with the requirements for a specific bearing system. It should allow, e.g., the reduction of the maximum temperatures in the lubricating film or power losses in modern design solutions of rotating machines.

The research ensures the issue of bearing design modification carried out so far, including the development of a numerical algorithm. Further research will enable the expanded identification of the static and dynamic characteristics of a wide multilobe bearings family.

REFERENCES

1. Someya T.: Journal-Bearing Databook, Springer-Verlag Berlin, Heidelberg 1989.
2. Strzelecki S.: Journal Bearings. Identification of the Operating Characteristics of Multilobe, Hydrodynamic Radial Bearings, Publishing House of the Silesian Univ. of Technology, Gliwice 2021.
3. Pinkus O.: Thermal Aspects of Fluid Film Tribology, Suffolk, Mech. Engrs., Publications Limited, ASME Press Series, 1991.
4. Strzelecki S.: An Effect of Lobe Profile on the Load Capacity of 2-Lobe Journal Bearing. Chinese Academy of Sciences, Mathematics Physics Astronomy. Series A Vol. 44, Supplement, August 2001. Science in China Press, pp. 94–100.
5. Dimofte F.: Wave Journal Bearing with Compressible Lubricant – Part I: The Wave Bearing Concept and a Comparison to the Plain Circular Bearing, Tribology Transactions 1995, Vol. 38, pp. 153–160.
6. Dettmar D., Kühl S., at al.: Advancement of a radial journal bearing for highest load capacity for big steam turbines for power generation. 7th IFToMM- Conference on Rotor Dynamics, September 25–28, Vienna 2006.
7. DeCamillo S.: Current issues regarding unusual conditions in high-speed turbomachinery. 5th EDF&LMS Workshop "Bearing Behaviour Under Unusual Operating Conditions". SP2MI-Futuroscope – 5 October, 2006. University of Poitiers, France. A.1 – 1.10.
8. Neale M.J.: The Tribology Handbook. Butterworth- Heinemann, Oxford 1995.
9. Olszewski O., Kiciński J., Strzelecki S.: Study on the applied solutions of main turbine bearings with the determination of the development direction of their design Part. I and II, Gdańsk University of Technology. November 1996. For the ABB Zamech, 1996 (in Polish).
10. Strzelecki S.: Multilobe journal bearings with different lobes geometry, 2018 (Author investigations – unpublished).
11. Strzelecki S.: Floating ring journal bearings of multilobe design in turbochargers. Scientific Automotive Conference KONMOT-2018. Sept. 13–14th, 2018 Krakow, Poland. Book of Abstracts, 2018, pp. 394––396.
12. Strzelecki S.: Dynamic characteristics of 4-lobe journal bearing with partial sliding surfaces, Warsaw University of Technology. Institute of Machine Design. XXIV FRENCH – POLISH MECHANICS SEMINAR. 17th of October 2016. MACHINE DYNAMICS RESEARCH, Vol. 36, No. 2, pp. 71–78.
13. Strzelecki S.: Effect of the sleeve profile on the stability of rotor operating in multilobe journal bearings. Proceedings of XXVII Symposium on Vibrations in Dynamical Systems, Vol. XXVII, 2016, pp. 339––346.
14. Ghoneam S.M., Strzelecki S.: Thermal Problems of Multilobe Journal Bearings Tribosystem. International Tribology Conference AIMETA, Rome, Italy 2004, pp. 533–540.
15. Strzelecki S., Socha Z.: Operating temperatures of the bearing system of grinding spindle, Tribologia 2010, nr 2 (236), pp. 157–167.
16. Strzelecki S.: Thermal Performances of 2-Lobe Journal Bearings, Tribologia 2007, No. 1 (211), pp. 185––198.
17. Strzelecki S., Brito G.C.Jr.: Power loss of tilting multi-pad, large overall dimensions journal bearings, Machine Dynamics Problems 2008, Vol. 32, No. 1, pp. 88–96.
18. Strzelecki S., Czaplicki Z.: Application of Multilobe Journal Bearings in the Design of Needle Punching Machine. 47th Textile Research Symposium. Book of Abstracts, Liberec, Czech Republic, The Textile Machinery Society of Japan TMSJ 2019, pp. 122–123.